Title

Assessing the carbon dioxide balance of a degraded tropical peat swamp forest following multiple fire events of different intensities

List of Authors:

Shinjiro Ohkubo[1], Takashi Hirano[1*], Kitso Kusin[2]

Correspondence: Takashi Hirano

E-mail address: hirano@env.agr.hokudai.ac.jp

Postal address: Research Faculty of Agriculture, Hokkaido University

Kita 9, Nishi 9, Kita-ku, Sapporo, 060-8589 Hokkaido, Japan.

Phone numbers: +81-11-706-3689

Institutional affiliations:

[1]Research Faculty of Agriculture, Hokkaido University, Sapporo 060-8589, Japan,

[2]CIMTROP, University of Palangkaraya, Palangkaraya 73112, Indonesia

Keywords:

CO_2 flux; coarse woody debris; drainage; eddy covariance technique; El Niño drought; groundwater level

Abstract:

Tropical peat swamp forest is a unique ecosystem rich in carbon and water, accumulating a huge amount of carbon as peat. However, the huge carbon pool has been threatened by oxidative peat decomposition and fire loss mainly because of deforestation and drainage. Fire causes acute carbon dioxide (CO_2) emissions through the combustion of biomass and peat. Also, fire should change the CO_2 balance of postfire ecosystems. Although it is crucial to quantify CO_2 balance even after a fire event to understand the total fire impact, information based on field measurement is lacking. Thus, we had measured eddy CO_2 flux above a repeatedly burned degraded peat forest for about 13 years since 2004. The site was a stable CO_2 source of 147−290 g C m^{-2} yr^{-1} for five years after a stand-replacing fire in 2002. Unexpectedly, a moderate-severity fire in 2009 changed the site to a CO_2 sink of about −600 g C m^{-2} yr^{-1}. The drastic change would have been caused by a large decrease in the decomposition of plant debris, which had accumulated since the 2002 fire but was burned by the 2009 fire. In contrast, gross primary production (GPP) remained about the same even though vegetation was damaged, mainly because year-round wet conditions caused by a La Niña event promoted the regrowth of hygrophilous herbaceous plants and were favorable to their GPP. The site also had a low-severity fire and was drained in 2014 but did not return to a CO_2 source. However, the net ecosystem CO_2 uptake after the 2009 fire was insufficient to recover a large amount of fire CO_2 emission. If CO_2 emissions from four fires in 1999, 2002, 2009 and 2014 are counted, the site is expected to owe an outstanding CO_2 debt of 25 kg C m^{-2}.

1. Introduction

Tropical peatlands are a huge soil carbon pool of 105 Gt C (Dargie *et al.*, 2017), of which 65% have accumulated in insular Southeast Asia, coexisting with peat swamp forest (Page *et al.*, 2011). In recent decades, however, peat swamp forest has experienced two major disturbances: land conversion and fire. Land conversion accompanied by deforestation is mainly to develop agricultural land, such as oil palm and acacia plantations. In Indonesia and Malaysia, peat swamp forest decreased by 7.3 Mha from 1990 to 2015, and consequently plantations and small holders' farmlands occupy more than 50% of tropical peatlands' area (Miettinen et al., 2016). Also, vast deforested area is left unused as secondary forests, shrublands and grasslands (Miettinen et al., 2016). Drainage is common practice in land conversion to lower the groundwater level (GWL), which potentially enhances oxidative peat decomposition and increases soil carbon dioxide (CO_2) efflux (e.g. Hirano et al., 2009; Sundari et al. 2012; Wakhid et al., 2017; Itoh et al., 2017).

Intact peat forest does not burn easily because of high GWL (Page and Hooijer, 2016). However, peat aridification due to drainage raises the risk of peat fire, especially in the dry season because dry peat is flammable. In forests on mineral soil, fire burns aboveground biomass (AGB) and plant debris (flaming). Besides flaming, peat can keep burning belowground (smoldering). Peat fire frequently occurs near drainages and reoccur there though burned peat depth decreases with fire recurrence (Konecny et al., 2016). In Indonesia, wildfires have occurred every year in the dry season (Gaveau et al., 2014). The fires enlarge in area and severity when an El Niño event occurs, because the event causes drought. Through biomass and peat burning, a large amount of CO_2 is emitted, and smoke produces haze. Large-scale haze covers maritime Southeast Asia and

causes economic damage and health problems (Page and Hooijer, 2016). In addition, haze diffuses and attenuates solar radiation incident on the ground, which affects gross primary production (GPP) (Kobayashi et al., 2005; Hirano et al., 2012; Stiegler et al., 2019). For instance, in 1997, when one of the strongest El Niño events occurred, the area of 9.7 Mha burned over Indonesia, of which peatlands occupied 15% (Murdiyarso and Adningsih, 2007), and CO_2 of 0.81–2.57 Gt C was emitted through biomass and peat burning (Page et al., 2002). In 2015, another strong El Niño year, large-scale fires burned 4.6 Mha over Indonesia, of which peatlands occupied 37%, and emitted 0.24 Gt C of CO_2 (Lohberger et al., 2017), accounting for 16% of the annual global CO_2 emissions through land-use change (Friedlingstein et al., 2019).

Fires severely disturb ecosystems and consequently change their carbon balance. Thus, in addition to estimating the large amount of pyrogenic CO_2 emission, it is essential to quantify the carbon balance of postfire ecosystems to assess how much carbon is lost in total by a fire event. Fire disturbances in peatlands include loss or degradation of vegetation, change in the amount of plant debris, loss of surface peat, change in peat properties and change in soil microbial community. The loss or degradation of vegetation decreases GPP and plant respiration, increases soil temperature (Hirano et al., 2014) and decreases evapotranspiration (Hirano et al., 2015) because of the decrease in the leaf area index (LAI). The amount of plant debris increases or decreases depending on fire severity and frequency (Hanula et al., 2012). When plant debris decreases, heterotrophic respiration can decrease, and vice versa. Surface peat is burned and lost especially by smoldering. As a result, recalcitrant deeper peat is exposed (Lupascu et al., 2020), and the peat surface subsides, which relatively raises GWL (Konecny et al., 2016) and might increase CH_4 emissions (Hirano et al., 2009). Thus, the peat loss potentially suppresses

93 oxidative peat decomposition. Fire burning also changes peat physicochemical properties,
94 including an increase in pH, bulk density and ash content and decrease in nitrogen and
95 organic carbon (Smith et al., 2001; Dikici and Yilmaz, 2006). The effects of these changes
96 on carbon cycles are complex and depend on fire severity and frequency (Neary et al.,
97 1999). Besides burning, fire makes soil organic matter (SOM) more stable by heating,
98 thereby reducing microbial respiration (Flanagan et al., 2020). In addition, burning affects
99 soil microbial community structure and can alter carbon-cycling processes (Ward et al.,
100 2012).

101 The overall CO_2 balance of postfire ecosystems has been measured by the eddy
102 covariance (EC) and chamber techniques, especially in mid and high latitudes. A
103 chronosequnce study using EC data showed that most forests in North America changed
104 to a large CO_2 source immediately after stand-replacing fires and returned to a CO_2 sink
105 in 10 years (Amiro et al., 2010). Another chronosequnce study using chamber data
106 showed that boreal bogs in Canada returned to a CO_2 sink in 13 years on average after
107 severe fires (Wieder et al., 2009). Severe fire changed forests and bogs to a CO_2 source
108 owing to a large decrease in GPP, whereas ecosystem respiration (RE) showed a small
109 change (Amiro et al., 2010; Dore et al., 2012; Wieder et al., 2009). Following gradual
110 GPP increase with vegetation regrowth after fire, net CO_2 uptake becomes positive
111 (Ueyama et al., 2019). In tropical peatland, only Hirano et al. (2012) reported the CO_2
112 balance of a burned degraded swamp forest. They showed that the degraded forest was a
113 stable CO_2 source during 1–5 years after a stand-replacing fire. However, all the above-
114 mentioned results are from stand-replacing or severe fires. Fire effects on ecosystem CO_2
115 balance should depend on combustion severity, but related information based on field
116 studies is lacking (Meigs et al., 2009).

We started measuring eddy CO_2 flux in a severely burned degraded peat swamp forest in Indonesia in 2004 (Hirano et al.,2012). The site was burned moderately again in 2009. Although many of regrowing trees survived, the measurement was forced to be suspended because of fire damage to the power system. We resumed the measurement after 2.5 months of suspension and continued it until the end of 2016. The site was lightly burned again and drained in 2014. In this study, we assessed the CO_2 balance of the degraded swamp forest and investigated the effects of multiple fire events of different intensities and drainage as well as El Niño / La Niña events on the CO_2 balance.

In Southeast Asia, it is projected that global warming will increase extreme drought occurrence during this century (Cai et al., 2014; Cai et al., 2015; Cook et al., 2020). In addition, human-induced disturbance on peatland hydrology will increase drought severity in Indonesia (Taufik et al., 2020). These predictions indicate that fire risk will increase in tropical peatlands. Thus, we must understand more about fire effects on tropical peatland CO_2 balance.

2. Materials and methods

2.1 Study site

The study site (2.34ºS, 114.04ºE) was in tropical peatland near Palangkaraya, Central Kalimantan, Indonesia, which was called DB in our previous paper (Hirano et al., 2012). The site was in Block C of ex-Mega Rice Project (Page et al., 2009) and used to be a selectively logged peat swamp forest with a peat depth of about 4 m but burnt repeatedly in 1997, 2002, 2009 and 2014, El Niño years. The forest was severely damaged by stand-replacing fire in 2002, leaving a few standing dead trees and a lot of coarse woody debris (CWD) on the ground (Fig. 1a). The thickness of burned peat by the 2002 fire was 0.22

141 m on average in the study site (Hirano et al., 2014). Peat probably burned also in 1997,
142 but no data were available on the combustion thickness. A large canal was excavated in
143 1996–1997 in the area and had functioned to drain the site (Page et al., 2009).
144 A 4-m-tall tower was built at about 200 m from the canal in April 2004. Fetches for
145 the west, south, north and east directions were 250, 300, 1000 and 1000 m, respectively.
146 In April 2004, 1.5 years after the 2002 fire, ferns (*Stenochlaena*, *Blechnum* and *Lygodium*
147 spp.) and sedge (*Cyperus*, *Scleria* and *Eleocharis* spp.) plants were sparsely distributed,
148 of which *Stenochlaena palustris* was dominant. The ground was studded with fire scars
149 with water (Fig. 1b). Fern and sedge plants had grown up to 0.5 m and covered most parts
150 of the ground in June 2005 (Fig. 1c). A few young trees had regenerated, and the canopy
151 height reached 0.8–0.9 m on average in 2009 before the next fire (Fig. 1d). A fire
152 moderately burned the study site in September 2009. Although stand replacement did not
153 occur, some trees died, and others defoliated. The aboveground part of herbaceous plants
154 burnt. A considerable amount of CWD on the ground burned out. The peat surface burned
155 in spots (Fig. 1e). Power cables and ground sensors were severely damaged. After the
156 moderately-severity fire, surviving trees started to foliate under high groundwater level
157 (GWL) conditions, and ferns and sedge plants rapidly regrew and covered most of the
158 ground in December 2009 (Fig. 1f). Sparsely existing young trees, which was dominated
159 by *Combretocarpus rotundatus,* kept growing with dense understory; the canopy height
160 exceeded 2 m in 2013 (Fig. 1g). In May–June 2014, a small canal with a width of about
161 1.5 m was excavated by the local community at about 100 m north of the tower and
162 lowered GWL (Fig. 2b). The study site was burned again by a light-severity fire in
163 September 2014. Just before the fire, tree density with a diameter at breast height (DBH)
164 > 3 cm was 860 trees ha^{-1}, and aboveground biomass (AGB) was 19.0 t ha^{-1}. The fire

burned herbaceous plants, litter accumulation on the ground and young trees in spots, though many trees survived from burning (Fig. 1h). In 2015, a strong El Niño year, although some fires occurred in the area, the site did not burn but was covered with dense smoke. The regrowth of herbaceous plants was slower after the 2014 fire than after the 2009 fire, probably because of lowered GWL by El Niño drought and canal excavation.

The mean annual temperature and precipitation measured at 1.5 m height for 2005–2016 were 26.4 ± 0.3℃ and 2640 ± 473 mm (mean ± 1 standard deviation (SD)), respectively. The dry season (monthly precipitation < 100 mm) usually lasts for 3–4 months between July and October. Between 2000 and 2016, El Niño events occurred in 2002–2003, 2004–2005, 2006–2007, 2009–2010, and 2014–2016, whereas La Niño events occurred in 2000–2001, 2005–2006, 2007–2008, 2008–2009, 2010–2012, and 2016 according to Oceanic Niño Index (NOAA; https://origin.cpc.ncep.noaa.gov/products/analysis_monitoring/ensostuff/ONI_v5.php).

2.2 Measurement of flux and environmental factors

Measurement was continuously conducted from April 2004 to December 2016, though flux data were available until October 25, 2016 because of sensor malfunction. Eddy CO_2 flux was measured using a sonic anemometer-thermometer (CSAT3; Campbell Scientific Inc., Logan, UT, USA) and an open-path CO_2/H_2O analyzer (LI7500; Li-Cor Inc.) using the EC technique at 3.0 m height (April 2004 to February 2011), 3.6 m (February 2011 to March 2012), 7.2 m (March 2012 to December 2013) or 13.6 m (after December 2013). The height was raised following tree growth. The flux sensors were separated by 0.2 m. Eddy signals were collected with a data logger (CR1000; Campbell Scientific Inc.) at 10 Hz. CO_2 concentration was also measured at heights of 0.4, 0.7, 1.5, 2.7, 5.7 and 13.6 m

189 in rotation with a closed-path CO_2 analyzer (LI820; Li-Cor Inc.) after December 2013.
190 Sampling height was switched every 30 seconds, and the mean for the last 5 s was
191 recorded with another datalogger (CR1000; Campbell Scientific Inc.). The two CO_2
192 analyzers were calibrated every three months using two standard gases.
193 Air temperature and relative humidity were measured using a platinum resistance
194 thermometer and a capacitive hygrometer (HMP45; Vaisala, Helsinki, Finland),
195 respectively, installed in a radiation shield (DTR503A; Vaisala) at 1.5 m height.
196 Additionally, air temperature and relative humidity were measured at 7.2 m from June
197 2012 to December 2013 or at 13.6 m from December 2013 to December 2016.
198 Precipitation was measured with a tipping-bucket rain gauge (TE525; Campbell Scientific
199 Inc.) at 1.5 m. Downward photosynthetic photon flux density (PPFD) was measured at
200 3.3 m (April 2004 to March 2012), 6.8 m (March 2012 to December 2013) or 13.6 m
201 (December 2013 to December 2016) with a quantum sensor (LI-190S; Li-Cor Inc. or
202 PQS1; Kipp & Zonen, Delft, The Netherland). Soil temperature at 5 cm depth was
203 measured at two points with thermocouple thermometers. These sensor signals were
204 collected every 10 s, and their half-hourly means were recorded with dataloggers
205 (CR1000 and CR10X; Campbell Scientific Inc.). GWL was measured half hourly with a
206 water level logger (DL/N; Sensor Technik Sirnach AG, Sirnach, Switzerland or DCX-22
207 VG; Keller AG, Winterthur, Switzerland) at a single point, avoiding fire scars. GWL was
208 relative groundwater level from the ground surface. When the water surface was
209 belowground, GWL was negative.
210 The measurement was suspended from September 20 to December 4, 2009 because of
211 power problems due to fire damage. For the suspension period, we substituted data
212 measured at the drained forest site (DF) about 600 m away from this site (Hirano et al.,

2012) for precipitation and PPFD, which were basically independent of ground conditions. Also, vapor pressure deficit (VPD), GWL and soil temperature, which were used for the gap filling of CO_2 fluxes, were estimated from the DF's data using significant linear relationships ($P < 0.001$). Linear regression was conducted for the period between September and December 2006 in another El Niño year; R^2 was 0.89 (VPD), 0.95 (GWL) and 0.48 (soil temperature).

2.3 Flux calculation and quality control

Half-hourly eddy CO_2 flux was calculated using Flux Calculator software (Ueyama et al., 2012) with the following procedures: (1) the removal of noise spikes (Vickers and Mahrt, 1997); (2) double rotation for tilt angles; (3) correction for high frequency loss (Massman, 2000; Massman, 2001); (4) correction for air density fluctuations (Webb et al., 1980). To avoid flow distortion by the tower, data with wind directions within 20° from the north were excluded; 19% of data were excluded in total. Data during rain were also removed. In addition, data beyond the range of mean ± 3 SDs (> 50 or < −50 μmol m^{-2} s^{-1}) were screened out as outliers. We checked the stationarity for each 30-min run (Foken and Wichura, 1996). We calculated difference between covariance values for the whole 30 min and the average of six 5-min covariance values. Data were excluded, when the difference was more than 100% (Foken et al., 2004).

The CO_2 storage change (FS) under the flux measurement height was calculated every three minutes from CO_2 concentrations measured at a height with the open-path analyzer before December 2013 or CO_2 profiles after December 2013, and then their mean and SD were calculated half hourly. The half-hourly mean FS was also quality-controlled using the SD by the same method as in Hirano et al. (2007, 2012). Net ecosystem CO_2 exchange

(NEE) was calculated as the sum of the eddy CO_2 flux and FS.

To exclude underestimated nighttime NEE under calm conditions, we examined the dependency of nighttime NEE on friction velocity (u_*) by the same method as in Hirano et al. (2007). As a result, the dependence was found only during the period after July 2014, probably because trees increased in height. Nighttime NEE with $u_* < 0.074$ m s^{-1} was excluded only after July 2014, which is defined later as Period III. Through all quality control procedures, 45 ± 19% and 61 ± 7% (mean ± 1 SD) of NEE data were missed in the daytime and nighttime, respectively, each year.

2.4 Gap-filling and partitioning of NEE

Missing NEE data were gap-filled by the lookup table method on a half-hourly basis. Lookup tables were created every two months using GWL and soil temperature for ecosystem respiration (RE), and PPFD and VPD for gross primary production (GPP). First, we extracted quality-controlled NEE data in the nighttime (PPFD < 5 μmol m^{-2} s^{-1}) as RE, including CO_2 emissions through burning. The RE data were binned equally into ten classes according to GWL, and then the data in each class were binned equally into three classes according to soil temperature and averaged. Using the lookup table, RE was estimated from GWL and soil temperature also in the daytime (PPFD ≥ 5 μmol m^{-2} s^{-1}). GPP was calculated as a difference between the measured daytime NEE and estimated daytime RE (= RE – NEE). The GPP was binned equally into ten classes by PPFD and then into three classes by VPD to create a lookup table. Thus, daytime NEE was gap-filled as a difference of estimated RE and GPP using the look-up tables.

2.5 Uncertainty in annual CO_2 fluxes

Considering the influence of the disturbances of fire and canal excavation, we divided the measurement period into three for the following analyses: Period I (before the 2009 fire; April 2004 to September 2009), Period II (after the 2009 fire until the canal excavation; December 2009 to June 2014) and Period III (after the canal excavation; July 2014 to December 2016). The annual values of RE, GPP and NEE were compared among three periods by one-way ANOVA and Tukey's HSD using a statistical software R (version 3.6.1).

Uncertainties due to random errors and gap-filling in annual RE, GPP and NEE were evaluated using the 24-h differencing approach (Hollinger and Richardson, 2005; Richardson et al., 2006; Richardson and Hollinger, 2007). Difference (δ) between two flux measurements exactly 24 hours apart was calculated as a random error (noise), if environmental conditions were similar within 75 μmol m^{-2} s^{-1} in PPFD, 3°C in air temperature, 1 m s^{-1} in wind speed and 2 hPa in VPD. In each of the three periods, δ was sorted according to NEE and binned equally into ten classes in positive and negative NEE ranges, respectively, and then SD of δ ($\sigma(\delta) = \sigma(x_1 - x_2)/\sqrt{2}$)) and mean NEE were calculated in each bin. The $\sigma(\delta)$, which is the random measurement uncertainty, was significantly correlated to mean NEE (Eq. 1) in each period ($P < 0.01$).

$$\sigma(\delta) = a + b|NEE| \quad (1)$$

where a and b are fitting parameters. Using the equation, $\sigma(\delta)$ was estimated from NEE. We conducted Monte Carlo simulations using R (version 3.6.1) to add a noise (δ) to each of half-hourly measured NEE according to a Laplace distribution, which was parameterized by β ($= \sigma/\sqrt{2}$) (Richardson and Hollinger, 2007). Using the data set of noise-added measured NEE, daytime RE and GPP were estimated, and RE, GPP and NEE were gap-filled by the look-up table method described above to calculate their annual

values. The Monte Carlo simulation was conducted 100 times, and the SD of the annual values were calculated as uncertainty due to random errors.

2.6 GPP parameters and peat decomposition

To understand the interannual variation of the relationship between GPP and PPFD, the following non-rectangular hyperbola (Thornley, 1976) was used as a fitting curve for half-hourly measured data in each year.

$$GPP = \frac{\alpha \cdot PPFD + GPP_{max} - \sqrt{(\alpha \cdot PPFD + GPP_{max})^2 - 4\alpha \cdot PPFD \cdot \theta \cdot GPP_{max}}}{2\theta} \quad (2)$$

where α is the initial slope of the fitting curve, GPP_{max} (μmol m^{-2} s^{-1}) the photosynthetic capacity at light saturation and θ the degree of curvature. To reduce the number of parameters, θ was set to be 0.8 (Johnson et al., 2010; Raj et al., 2016). The other two parameters (α and GPP_{max}) were determined using R (version 3.6.1).

CO_2 emissions through oxidative peat decomposition (PD; μmol m^{-2} s^{-1}) were estimated from GWL (m) using the following equation, which was determined from soil chamber data at this study site (Hirano et al., 2014).

$$PD = 1.48 \cdot ln(1.48 - 5.96 \cdot GWL) \quad (3)$$

2.7 Vegetation index and fire hotspots

The enhanced vegetation index (EVI) in moderate resolution imaging spectroradiometer (MODIS) data (MOD13Q1 Version 6) was downloaded from Land Processes Distributed Active Archive Center (https://lpdaac.usgs.gov/products/mod13q1v006/). Pixel data covering our site were used

as vegetation information, such as a proxy of AGB (Anaya et al., 2009; Huete et al., 2002). The data were composited every 16 days at 250 m spatial resolution. Also, MODIS hotspot data (MODIS Collection 6) acquired from the Fire Information for Resources Management System (https://firms.modaps.eosdis.nasa.gov/) were used to know the fire occurrence.

3. Results

3.1 Time-series variations

Precipitation showed a clear seasonal variation, except in 2008 and 2010, La Niña years (Fig. 2a). Following the seasonal precipitation variation, GWL showed a negative peak at the end of the dry season (Fig. 2b). The lowest monthly mean GWL was -0.92 m in 2006 and -1.38 m in 2015 before and after the canal excavation (Table 1). During the mid-wet season, typically between January and April, groundwater rose aboveground (GWL > 0 m) until 2014. In 2010, however, there was no dry month, and consequently GWL was stable at around 0 m throughout the year. In addition, GWL remained below the peat surface (< -0.17 m monthly) even in the rainy season after canal excavation in 2014. In comparison between 2011 and 2016, which had similar annual precipitation (Table 1), annual mean GWL was lower by 0.38 m in 2016 after drainage. Fire occurred in the dry season when GWL lowered. Many hotspots were detected in 2002, 2009, 2014, and 2015, El Niño years (Fig. 2g). The number of hotspots within a 5-km radius from the tower were 442, 262, 117 and 80, respectively, in 2002, 2009, 2014 and 2015; the shortest distances from the tower were 0.15 (2002), 0.19 (2009), 0.26 (2014) and 1.23 km (2015). In 2002, EVI drastically decreased from 0.61 to 0.12 (Fig. 2f). EVI also dropped to 0.28 by the 2009 fire and had gradually recovered toward the pre-fire level of 0.51. In contrast,

fire decrease in EVI was temporary for about 10 months in 2014. PPFD decreased in the dry seasons of 2002, 2006, 2009, 2014 and 2015 because of dense smoke emitted from fires (Fig. 2c). Daytime VPD increased in the dry season every year except in 2008 and 2010, La Niña years (Fig. 2d). The VPD peak became high in El Niño years, especially in 2009, 2014 and 2015.

Before the 2009 fire, RE was almost stable with small monthly fluctuations, whereas GPP had gradually increased following vegetation regrowth (Figs. 2e and 2f). During the period, NEE was positive except for a few months. In December 2009, 2.5 months after the fire, RE decreased to less than half of the pre-fire level. By contraries, there was little change in GPP even after the fire. As a result, NEE drastically changed from positive to negative. Both RE and GPP were almost stable in 2010, and then started increasing following gradual EVI increase (Fig. 2f). During the fire in 2014, RE showed a sharp peak because of a large amount of CO_2 emission through burning in the study site (Fig. 1h). In contrast, GPP suddenly decreased by 2.8 g C m^{-2} d^{-1} between August and November (Fig. 2e). These opposite changes resulted in a large NEE peak. After the fire, RE rapidly decreased to less than the pre-fire level, whereas GPP slightly recovered, resulting in a CO_2 neutral (NEE ≅ 0 g C m^{-2} yr^{-1}) in 2015. In 2016, NEE returned to be negative (Table 1).

3.2 Environmental responses of RE and GPP

Generally, RE decreased with increasing GWL in all periods (Fig. 3a). In Period I, RE showed a decreasing tendency only when GWL was positive. In contrast, RE decreased with increasing GWL over the whole GWL range in Period II, though the range was narrower than those of the other periods. If excluding the spiky RE during the fire in

356 September and October 2014 (Fig. 2e), RE showed a clear negative relationship with
357 GWL in Period III. To examine more about RE response to GWL, we estimated the sum
358 of autotrophic respiration and the decomposition of CWD and litter accumulation on the
359 ground by subtracting estimated PD (Eq. 2) from the measured RE (RE – PD). Positive
360 relationships were found between RE−PD and GWL in Periods I and III, if spiky fire data
361 were excluded (Fig. 3b); sensitivity to GWL was higher in Period I. RE was almost stable
362 until 2009 (Period I) in high GWL conditions (GWL ≥ −0.2 m) (Fig. 4). After the fire, RE
363 at high GWL decreased by half in 2010, then had increased until 2014.
364 GPP_{max} increased from 2004 to 2005, and then became almost stable until 2009 (Fig.
365 5). After the 2009 fire, GPP_{max} kept increasing until 2012 and decreased in 2015. To
366 examine the influence of VPD, light-saturated GPP at PPFD ≥ 1000 μmol m^{-2} s^{-1}
367 (GPP_{1000}) was plotted against VPD for the three periods under different GWL conditions
368 (Fig. 6). In Period I, GPP_{1000} decreased gently but linearly with increasing VPD regardless
369 of GWL conditions. In Periods II and III, however, GPP_{1000} started decreasing at VPD of
370 about 15 hPa. Larger data scattering at GWL < −0.4 m in Period II and GWL ≥ −0.1 m in
371 Period III is due to smaller data size. The relationship of GPP_{1000} with VPD was
372 independent of GWL conditions.
373
374 **3.3 Annual NEE, RE and GPP**
375 Annual NEE was positive over 150 g C m^{-2} yr^{-1} for consecutive five years until 2009
376 (Table 1). After 2010, annual NEE drastically decreased to less than −570 g C m^{-2} yr^{-1}
377 mainly because of the large decrease in RE. The fire halved annual RE from 1488 to 715
378 g C m^{-2} yr^{-1}, whereas annual GPP decreased only by 49 g C m^{-2} yr^{-1} from 2008 to 2010.
379 The decrease in RE–PD (718 g C m^{-2} yr^{-1}) contributed much more to the RE decrease

than PD decrease (55 g C m^{-2} yr^{-1}). After the fire, NEE continued to increase negatively until 2013 because GPP increased more rapidly than RE; increases between 2010 and 2013 were 628 and 735 g C m^{-2} yr^{-1}, respectively, in RE and GPP. In 2014, GWL was clearly decreased by canal excavation and less precipitation, and fire occurred in the study site. As a result, NEE changed to almost zero (-28 g C m^{-2} yr^{-1}) because of a large increase in RE and a slight decrease in GPP. The large RE increase was attributable to fire CO_2 emissions. The neutral NEE continued until 2015.

To examine the large change of CO_2 fluxes, annual values were averaged in the three periods: 2005–2008, 2010–2013 and 2015–2016 (Table 2). Their interannual variations (1 SD) in each period were greater than uncertainties due to random errors (Table 1). Although a significant difference was not found in GPP (Table 2), RE and NEE were significantly smaller or more negative in 2010–2013 ($P < 0.05$).

We have already reported the CO_2 balance of this site between 2004 and 2009 (Hirano et al., 2012), in which annual periods began in early June. Using the same annual periods, annual CO_2 fluxes were calculated and compared for five years. As a result, annual NEE of this study (277 ± 113 g C m^{-2} yr^{-1}) was smaller than that of Hirano et al. (2012) by 185 g C m^{-2} yr^{-1} on average. This difference was mainly due to RE difference of 233 g C m^{-2} yr^{-1}, which was mainly caused by data screening in the nighttime. In Hirano et al. (2012), negative data or data > 100 μmol m^{-2} s^{-1} were excluded in the nighttime at the beginning of quality control procedures. In contrast, screening criteria were between −50 and 50 μmol m^{-2} s^{-1} both in the daytime and nighttime in this study. The biased screening overestimated RE in Hirano et al. (2012). Thus, we can say that this study is fairer in quality control and more reliable.

4. Discussion

4.1 Ecosystem respiration

The RE drastically decreased after the 2009 fire (Fig. 2e). Annual RE was smaller by 773 g C m^{-2} yr^{-1} in 2010 than in 2008 (Table 1). In both years, La Niña events occurred, and GWL was high at around the ground surface throughout the year (Fig. 2b). As a result, the difference in the annual PD was small (55 g C m^{-2} yr^{-1}). Thus, the large difference in RE was due to decreases in autotrophic respiration and other heterotrophic respiration from CWD and litter accumulation on the ground, which were equivalent to RE–PD. The 2009 fire burned most of litter and CWD produced by the previous 2002 fire (Fig. 1e), leaving some charred CWD. Charred CWD is slow in decomposition (Deluca and Aplet, 2008; Donato et al., 2009). The RE–PD showed a large decrease after the 2009 fire at high GWL (Fig. 3b). These facts indicate that CO_2 efflux through the decomposition of CWD and litter accumulation sharply decreased.

Smoldering occurred only at some spots during the 2009 fire, but the peat surface burned along with litter accumulation. Such combustion processes replace labile carbon compounds with more recalcitrant charcoal (Milner, 2013). Even if peat does not burn, fire can thermally alter the chemistry of SOM and increase stable soil carbon, which potentially lowers the peat decomposition (Flanagan et al., 2020). Meanwhile, peat combustion increases mineral nutrient, pH and bulk density (Dikici and Yilmaz, 2006; Smith et al., 2001). Higher pH potentially enhances soil microbial activity and consequently increases microbial respiration (Moilanen et al., 2012). The effects of theses pyrogenic changes in peat properties depend on fire severity and frequency (Neary et al., 1999). Here, the decreasing effects possibly surpassed the increasing effects on carbon emissions.

After 2010, RE had gradually increased until the next fire in 2014 (Fig. 2e). During this period, the vegetation recovered with litter accumulation, as shown by EVI increase (Fig. 2f). PD was relatively stable under continuous higher GWL conditions (Table 1, Fig. 2b). Thus, the RE increase was attributable to the increase in autotrophic respiration and litter decomposition. GWL lowered to a large extent after 2014 because of canal excavation and El Niño drought (Fig. 2b). Even in the wet season, GWL remained belowground. As a result, PD increased rapidly up to 844 g C m^{-2} yr^{-1} in 2015 (Table 1). Eq. 3 to estimate PD was parameterized using the data measured in 2004–2006, in which GWL was higher than −0.9 m (Hirano et al., 2014). Thus, PD in 2015 with the minimum daily GWL of −1.53 m was extrapolated, and the annul PD might be overestimated (Itoh et al., 2017).

4.2 Gross primary production

The annual GPP decreased only by 49 g C m^{-2} yr^{-1} between 2008 and 2010 despite 30% decrease in EVI (Table 1). After 2010, GPP continued to increase until the 2014 fire (Fig. 2e) with the rapid regrowth of fern and sedge plants dominated by *Stenochlaen palustris*, which is typically growing in permanently damp open places (Chambers, 2013). The annual GPP in 2013 was 2027 g C m^{-2} yr^{-1}, which accounts for about 60% of that of a nearby peat swamp forest (UF site) (Hirano et al., 2012). The rapid regrowth was most probably due to limited GWL lowering (Fig. 2b). In 2010 immediately after the fire, GWL remained high throughout the year because of a La Niña event; daily mean GWL lowered only to -0.12 m. Thus, the hygrophilous fern and sedge plants could steadily recover with little water stress under sparse overstory. The leaf color usually gets lighter in the dry season because of desiccation, but little color change was found in 2010–2013. In addition,

452 wood and plant ashes would have promoted vegetation regrowth by increasing plant
453 available nutrients (Neary et al., 1999). Also, higher PPFD and lower daytime VPD
454 increased GPP and enhanced plant growth. Light-saturated GPP showed a decreasing
455 tendency with VPD when VPD was higher than 15 hPa (Fig. 6). Such a dry condition
456 occurred less frequently in 2010–2013 (Table 1). A rapid increase in GPP_{max} during this
457 period (Fig. 5) reflects the rapid vegetation regrowth and lower VPD, which was
458 favorable to GPP.

459 After 2014, canal excavation and an El Niño event dried the site, which lowered GWL
460 and raised VPD. In addition, aboveground vegetation was patchily damaged by the 2014
461 fire, and PPFD was attenuated sharply in 2015 by dense smoke emitted from surrounding
462 fires. As a result, both the annual GPP and GPP_{max} temporarily decreased in 2015, and
463 then recovered in 2016 with the disappearance of the El Niño event and vegetation
464 recovery (Table 1). The canal effect on GPP by GWL lowering was unclear because El
465 Niño drought and fire occurred concurrently.

466

467 **4.3 Fire emissions**

468 In 2014, large positive CO_2 flux had been measured for about 40 days in September
469 and October (Fig. 2e), when fire occurred in the study site. The large CO_2 efflux should
470 have included fire CO_2 emissions. The fire emissions were estimated to be 308 g C m^{-2}
471 as a difference between measured RE and estimated RE using look-up tables created
472 before and after the fire. AGB immediately before the fire was 19.0 t ha^{-1}. From an
473 emission factor (EF) of 0.45, which was an average for tropical forest (Akagi et al., 2011),
474 the fire emission of 19.0 t ha^{-1} corresponds to 36% combustion of AGB (Fig. 1h), if CWD
475 and litter did not burn. Through the fire, EVI decreased by about 40% (Fig. 2f).

476 Fire emissions were not measured in 2009, since the flux measurement was suspended.
477 We presumed that AGB before fire was almost the same in 2009 and 2014, because EVI
478 was at the same level (Fig. 2f). We also presumed that AGB burned by 50% through the
479 2009 fire, because EVI decreased by about 50%. Toriyama et al. (2014) conducted a forest
480 survey in the same area and reported that 86 t ha^{-1} of deadwood remained on average in
481 regenerating forests after the 1997 fire. Thus, we presumed that the same amount of CWD
482 remained in the study site and all the CWD burnt out in 2009. Using the EF of 0.45, fire
483 emission was estimated to be 4.30 kg C m^{-2} (= (19 × 0.5 + 86) × 0.45).
484 We also estimated fire emissions by fires in 1997 and 2002. In this area, AGB of peat
485 swamp forest was estimated to be 169 t ha^{-1} on average (Hayashi et al., 2015). According
486 to Toriyama et al. (2014), deadwood in mature forests accounts for 15% of AGB and 86
487 t ha^{-1} of deadwood remained after the 1997 fire. On the presumption that all the fuel mass
488 except the 86 t ha^{-1} of deadwood was burned by the two fires, fire emission was calculated
489 to be 4.88 kg C m^{-2} (= (169 + 169 × 0.15 − 86) × 0.45) using the same EF, though some
490 AGB was left unburned as CWD. Thus, the calculation should be overestimated, but it
491 can be compensated with the underestimation of the 2009 fire emissions. In addition, peat
492 was burned by 22 cm by the 2002 fire. The bulk density and carbon content of shallow
493 peat (0–25 cm) were 173 kg m^{-3} and 53.2% on average, respectively, in the study site
494 (Itoh et al., 2017). Although the peat properties were measured in 2014 after the 2009 fire,
495 these apply probably to the peat of 2002. Using another EF of 0.46 determined from
496 Indonesian peat with carbon content of 54.7% (Christian et al., 2003), CO_2 emission
497 through peat combustion was estimated to be 17.5 kg C m^{-2} (= 0.22 × 173 × 0.46). The
498 sum (22.4 kg C m^{-2}) of the two emissions from AGB and peat was total fire emissions.
499 The emissions accounted for about 70% of mean fire emissions from peatlands burned in

1997 in Central Kalimantan, Indonesia (Page et al., 2002).

4.4 Carbon dioxide balance

This study site was a constant CO_2 source until 2009 after a stand-replacing fire with smoldering in 2002. Unburned forest and wetland generally change from a CO_2 sink to a source by severe fire owing to the large decrease in GPP (Amiro et al., 2010; Dore et al., 2012; Ueyama et al., 2019; Wieder et al., 2009). In contrast, a moderate-severity fire in 2009 changed this site from a CO_2 source to a net annual CO_2 sink because of a large RE decrease with little GPP decrease (Table 1). The annual NEE of −615 g C m^{-2} yr^{-1} in 2010–2013 (Table 2) was much more negative than that (−403 g C m^{-2} yr^{-1}) of tropical humid evergreen forest (Luyssaert et al., 2007).

A complete carbon balance assessment of tropical peatlands with high GWL requires accounting for methane (CH_4) emissions. Hirano et al. (2009) measured CH_4 flux on the peat surface in the same area as this study site between 2004 and 2006 by the chamber method and showed a sigmoid relationship between CH_4 flux and GWL. Using the equation on the assumption that parameters were unchanged even after fires and drainage, we estimated CH_4 flux from GWL throughout the study period. As a result, annual CH_4 emissions were estimated to be 1.68 ± 0.30, 1.90 ± 0.36 and 0.14 ± 0.19 g CH_4 m^{-2} yr^{-1} on average, respectively, in 2005−2008, 2010−2013 and 2015−2016, which can be converted into 47.6, 53.2 and 3.9 g CO_{2eq} m^{-2} yr^{-1}, respectively, using a global warming potential (GWP) of 28 over a timescale of 100 years (IPCC, 2013). The result indicates that CH_4 emissions did not significantly change after the 2009 fire but significantly decreased ($P < 0.01$ according to Tukey's HSD) after the canal excavation in Period III because of low GWL.

524 Fluvial organic carbon flux is another essential component in the carbon balance of
525 peat ecosystems. Moore et al. (2013) estimated annual fluxes of dissolved organic carbon
526 (DOC) and particulate organic carbon (POC) as the product of their concentrations and
527 discharge in canals in intact peat swamp forest and drained disturbed peat swamp forest
528 in this study area. They reported that the annual total organic carbon (DOC + POC) flux
529 depended mainly on annual discharge. Annual total organic carbon flux was larger in the
530 drained forest because of larger annual discharge, whereas mean concentrations were
531 similar in the intact and drained forests. In our site since canal excavation lowered GWL
532 in 2014 (Fig. 2), discharge should have increased, and consequently fluvial organic
533 carbon flux increased temporarily in this transitional period. Alternatively, latent heat flux
534 normalized by net radiation did not change between Period II and III (Ohkubo et al., under
535 review), indicating that evapotranspiration capacities were almost the same in both
536 periods. Thus, if GWL keeps lowering after drainage, fluvial carbon loss would increase
537 owing to discharge increase. However, if GWL remains stable even at a low level, no
538 more increase in fluvial carbon flux would occur.
539 Cumulative CO_2 emissions, including fire emissions, had been decreasing after the
540 2009 fire until canal excavation and fire in 2014 because of the large negative NEE (Fig.
541 7). However, cumulative CO_2 were not compensated in 13 years; it was still positive at
542 about 3 kg C m^{-2} at the end of 2016. Although the moderate-severity fire significantly
543 changed the annual CO_2 balance of the repeatedly burned peatland, the change was
544 insufficient to recover the acute fire emissions in this period. In addition, if CO_2 emissions
545 from fires in 1999 and 2002 (22.4 kg C m^{-2}) is added, cumulative CO_2 emissions increase
546 up to 25.4 kg C m^{-2} at the end of 2016. If annual NEE (−615 g C m^{-2} yr^{-1}) in 2010–2013
547 (Table 2) continues, the cumulative CO_2 emissions can be compensated in about 40 years,

548 but is this possible? The site has already been drained since 2014. Lowered GWL
549 potentially enhances oxidative peat decomposition and increases fire risk (Konecny et al.,
550 2016). Thus, it should be impossible for the site to recover the total CO_2 emitted by fires.
551 This site was converted to an oil palm plantation soon after the flux monitoring was closed.
552 Although fire risk is expected to be low in plantations, oil palm plantations established
553 on peat have a potential to be a large CO_2 source up to 1 kg C m^{-2} yr^{-1} because of
554 insufficient peat compaction during land preparation (Kiew et al., 2020).
555 The study area was heavily degraded by deforestation and drainage through Mega Rice
556 Project (MRP) (Page et al. 2009). After MRP was terminated at the end of the 1990s, the
557 area has been abandoned and burned repeatedly. As a result, in Block B (4490 km^2) of
558 ex-MRP, non-woody vegetation area dominated by ferns like this study site occupied 36%
559 in 2005 (Hoscilo et al., 2011). Thus, this study can contribute to quantifying the CO_2
560 balance of degraded peatland on a regional scale. However, our result might not apply to
561 other degraded sites because postfire CO_2 balance depends on various conditions, such as
562 fire severity, disturbance histories and the hydrological environment. The drastic change
563 of CO_2 balance was probably caused by an appropriate combination of a moderately-
564 severity fire and consecutive year-round high GWL due to a La Niña event, which was
565 favorable to the rapid regrowth of herbaceous plants and their GPP. More field data
566 measured in various conditions are necessary in collaboration with a modeling approach
567 to robustly assess the CO_2 balance of degraded peat ecosystems.
568
569 **5. Conclusions**
570 The study site burnt two times in 2009 and 2014 and was drained by a canal excavated
571 in 2014 during the study period of about 13 years. Although fire damages were caused by

572 the El Niño drought, the second fire was probably triggered by drainage. In addition, the
573 smoke emitted by nearby fire attenuated PPFD considerably. On the other hand, the rainy
574 weather caused by La Niño events kept GWL high around the ground surface throughout
575 the year. These human and natural disturbances affected CO_2 fluxes compositely.

576 The large decrease in RE after the 2009 fire was probably due to a large decrease in
577 heterotrophic respiration from CWD and litter accumulation. A La Niña event
578 immediately after the fire produced a favorable wet condition for herbaceous plants'
579 regrowth and prevented PPFD attenuation due to smoke emissions from fire, which
580 increased GPP. As a result, the degraded peat swamp forest changed from a CO_2 source
581 to a sink. In 2014–2015, unfavorable events of canal construction, El Niño drought and
582 fire occurred concurrently. Consequently, GWL lowered, VPD increased, PPFD
583 decreased, and vegetation was patchily damaged. These events changed NEE, but the
584 study site did not return to a CO_2 source. However, the net ecosystem CO_2 uptake was
585 quite insufficient to recover a large amount of fire CO_2 emissions.

586

587 **Acknowledgements**

588 This study was supported by JSPS Core University Program, JSPS KAKENHI Grant
589 Numbers 13375011, 15255001, 18403001, 21255001, 25257401 and 19H05666, the JST-
590 JICA Project (SATREPS) (Wild Fire and Carbon Management in Peat-Forest in
591 Indonesia) and Technology Development Fund (no. 2-1504) by the Environmental
592 Restoration and Conservation Agency and the Ministry of the Environment, Japan. We
593 thank the late Dr. Suwido Limin for the site establishment and Drs. Yosuke Okimoto,
594 Kiwamu Ishikura, Masayuki Itoh and the staff of CIMTROP for their assistance in field
595 work. We also express our gratitude to the providers of burned fraction datasets of GFED.

We acknowledge the use of data from FIRMS operated by NASA's Earth Science Data and Information System (ESDIS) with funding provided by NASA Headquarters.

References

Akagi, S. K., Yokelson, R. J., Wiedinmyer, C., Alvarado, M. J., Reid, J. S., Karl, T., ... & Wennberg, P. O. (2011). Emission factors for open and domestic biomass burning for use in atmospheric models. *Atmospheric Chemistry and Physics*, 11(9), 4039-4072.

Amiro, B. D., Barr, A. G., Barr, J. G., Black, T. A., Bracho, R., Brown, M., ... & Dore, S. (2010). Ecosystem carbon dioxide fluxes after disturbance in forests of North America. *Journal of Geophysical Research: Biogeosciences*, 115, GK00K02, doil:10.1029/2010JG001390.

Anaya, J. A., Chuvieco, E., & Palacios-Orueta, A. (2009). Aboveground biomass assessment in Colombia: A remote sensing approach. *Forest Ecology and Management*, 257(4), 1237-1246.

Cai, W., Borlace, S., Lengaigne, M., Van Rensch, P., Collins, M., Vecchi, G., ... & England, M. H. (2014). Increasing frequency of extreme El Niño events due to greenhouse warming. *Nature Climate Change*, 4(2), 111-116.

Cai, W., Santoso, A., Wang, G., Yeh, S. W., An, S. I., Cobb, K. M., ... & Lengaigne, M. (2015). ENSO and greenhouse warming. *Nature Climate Change*, *5*(9), 849-859.

Chambers, T. C. (2013). A review of the genus *Stenochlaena* (Blechnaceae, subfamily Stenochlaenoideae). *Telopea*, 15, 13-36.

Christian, T. J., Kleiss, B., Yokelson, R. J., Holzinger, R., Crutzen, P. J., Hao, W. M., ... & Ward, D. E. (2003). Comprehensive laboratory measurements of biomass-burning emissions: 1. Emissions from Indonesian, African, and other fuels. *Journal of*

620 *Geophysical Research: Atmospheres*, 108(D23), 4719, doi:10.1029/2003JD003740.
621 Cook, B. I., Mankin, J. S., Marvel, K., Williams, A. P., Smerdon, J. E., & Anchukaitis, K.
622 J. (2020). Twenty-First Century Drought Projections in the CMIP6 Forcing
623 Scenarios. *Earth's Future*, 8, e2019EF001461. https://doi.org/10.1029/2019EF001461.
624 Dargie, G. C., Lewis, S. L., Lawson, I. T., Mitchard, E. T., Page, S. E., Bocko, Y. E., &
625 Ifo, S. A. (2017). Age, extent and carbon storage of the central Congo Basin peatland
626 complex. *Nature*, 542(7639), 86-90.
627 DeLuca, T. H., & Aplet, G. H. (2008). Charcoal and carbon storage in forest soils of the
628 Rocky Mountain West. *Frontiers in Ecology and the Environment*, 6(1), 18-24.
629 Dikici, H., & Yilmaz, C. H. (2006). Peat fire effects on some properties of an artificially
630 drained peatland. *Journal of environmental quality*, 35(3), 866-870.
631 Donato, D. C., Campbell, J. L., Fontaine, J. B., & Law, B. E. (2009). Quantifying char in
632 postfire woody detritus inventories. *Fire Ecology*, 5(2), 104-115.
633 Dore, S., Montes-Helu, M., Hart, S. C., Hungate, B. A., Koch, G. W., Moon, J. B., ... &
634 Kolb, T. E. (2012). Recovery of ponderosa pine ecosystem carbon and water fluxes
635 from thinning and stand-replacing fire. *Global change biology*, 18(10), 3171-3185.
636 Flanagan, N. E., Wang, H., Winton, S., & Richardson, C. J. (2020). Low-severity fire as
637 a mechanism of organic matter protection in global peatlands: Thermal alteration slows
638 decomposition. *Global Change Biology*, 26, 3930-3946.
639 Foken, T., & Wichura, B. (1996). Tools for quality assessment of surface-based flux
640 measurements. *Agricultural and forest meteorology*, 78(1-2), 83-105.
641 Foken, T., Göckede, M., Mauder, M., Mahrt, L/, Amiro, B., & Munger, W. (2004). Post-
642 field data quality control, In: Lee, X., Massman, W., & Law, B. (Eds.), Handbook of
643 Micrometeorology. Kluwer Academic Publishers, Dordrecht, pp. 181-208.

644 Friedlingstein, P., Jones, M., O'sullivan, M., Andrew, R., Hauck, J., Peters, G., ... &
645 DBakker, O. (2019). Global carbon budget 2019. *Earth System Science Data*, 11(4),
646 1783-1838.
647 Gaveau, D. L., Salim, M. A., Hergoualc'h, K., Locatelli, B., Sloan, S., Wooster, M., ... &
648 Verchot, L. (2014). Major atmospheric emissions from peat fires in Southeast Asia
649 during non-drought years: evidence from the 2013 Sumatran fires. *Scientific reports*, *4*,
650 6112.
651 Hanula, J. L., Ulyshen, M. D., & Wade, D. D. (2012). Impacts of prescribed fire frequency
652 on coarse woody debris volume, decomposition and termite activity in the longleaf
653 pine flatwoods of Florida. *Forests*, 3(2), 317-331.
654 Hayashi, M., Saigusa, N., Yamagata, Y., & Hirano, T. (2015). Regional forest biomass
655 estimation using ICESat/GLAS spaceborne LiDAR over Borneo. *Carbon*
656 *management*, 6(1-2), 19-33.
657 Hirano, T., Segah, H., Harada, T., Limin, S., June, T., Hirata, R., & Osaki, M. (2007).
658 Carbon dioxide balance of a tropical peat swamp forest in Kalimantan,
659 Indonesia. *Global Change Biology*, 13(2), 412-425.
660 Hirano, T., Jauhiainen, J., Inoue, T., & Takahashi, H. (2009). Controls on the carbon
661 balance of tropical peatlands. *Ecosystems*, 12(6), 873-887.
662 Hirano, T., Segah, H., Kusin, K., Limin, S., Takahashi, H., & Osaki, M. (2012). Effects
663 of disturbances on the carbon balance of tropical peat swamp forests. *Global Change*
664 *Biology*, 18(11), 3410-3422.
665 Hirano, T., Kusin, K., Limin, S., & Osaki, M. (2014). Carbon dioxide emissions through
666 oxidative peat decomposition on a burnt tropical peatland. *Global change*
667 *biology*, 20(2), 555-565.

668 Hirano, T., Kusin, K., Limin, S., & Osaki, M. (2015). Evapotranspiration of tropical peat
669 swamp forests. *Global change biology*, *21*(5), 1914-1927.
670 Hollinger, D. Y., & Richardson, A. D. (2005). Uncertainty in eddy covariance
671 measurements and its application to physiological models. *Tree Physiology*, 25, 873-
672 885.
673 Hoscilo, A., Page, S. E., Tansey, K. J., & Rieley, J. O. (2011). Effect of repeated fires on
674 land-cover change on peatland in southern Central Kalimantan, Indonesia, from 1973
675 to 2005. *International Journal of Wildland Fire*, 20, 578-588.
676 Huete, A., Didan, K., Miura, T., Rodriguez, E. P., Gao, X., & Ferreira, L. G. (2002).
677 Overview of the radiometric and biophysical performance of the MODIS vegetation
678 indices. *Remote sensing of environment*, 83(1-2), 195-213.
679 IPCC (2013). Climate Change 2013: The Physical Science Basis. Cambridge University
680 Press, Cambridge.
681 Itoh, M., Okimoto, Y., Hirano, T., & Kusin, K. (2017). Factors affecting oxidative peat
682 decomposition due to land use in tropical peat swamp forests in Indonesia. *Science of*
683 *the Total Environment*, 609, 906-915.
684 Johnson, I. R., Thornley, J. H., Frantz, J. M., & Bugbee, B. (2010). A model of canopy
685 photosynthesis incorporating protein distribution through the canopy and its
686 acclimation to light, temperature and CO_2. *Annals of botany*, 106(5), 735-749.
687 Kiew, F., Hirata, R., Hirano, T., Xhuan, W. G., Aries, E. B., Kemudang, K., ... & Melling,
688 L. (2020). Carbon dioxide balance of an oil palm plantation established on tropical
689 peat. *Agricultural and Forest Meteorology*, 295, 108189.
690 Kobayashi, H., Matsunaga, T., & Hoyano, A. (2005). Net primary production in Southeast
691 Asia following a large reduction in photosynthetically active radiation owing to

692 smoke. *Geophysical Research Letters*, 32(2), L02403, doi:10.1029/2004GL021704.
693 Konecny, K., Ballhorn, U. W. E., Navratil, P., Jubanski, J., Page, S. E., Tansey, K., ... &
694 Siegert, F. (2016). Variable carbon losses from recurrent fires in drained tropical
695 peatlands. *Global Change Biology*, 22(4), 1469-1480.
696 Lohberger, S., Stängel, M., Atwood, E. C., & Siegert, F. (2017). Spatial evaluation of
697 Indonesia's 2015 fire-affected area and estimated carbon emissions using Sentinel-
698 1. *Global change biology*, 24(2), 644-654.
699 Lupascu, M., Akhtar, H., Smith, T. E., & Sukri, R. S. (2020). Post-Fire carbon dynamics
700 in the tropical peat swamp forests of Brunei reveal long term elevated CH4 flux. *Global*
701 *Change Biology*, 26, 5125-5145.
702 Luyssaert, S., Inglima, I., Jung, M., Richardson, A. D., Reichstein, M., Papale, D., ... &
703 Aragao, L. E. O. C. (2007). CO_2 balance of boreal, temperate, and tropical forests
704 derived from a global database. *Global change biology*, 13(12), 2509-2537.
705 Massman, W. J. (2000). A simple method for estimating frequency response corrections
706 for eddy covariance systems. *Agricultural and Forest Meteorology*, 104(3), 185-198.
707 Massman, W. J. (2001). Reply to comment by Rannik on" A simple method for estimating
708 frequency response corrections for eddy covariance systems". *Agricultural and Forest*
709 *Meteorology*, 107, 247-251.
710 Meigs, G. W., Donato, D. C., Campbell, J. L., Martin, J. G., & Law, B. E. (2009). Forest
711 fire impacts on carbon uptake, storage, and emission: the role of burn severity in the
712 Eastern Cascades, Oregon. *Ecosystems*, 12(8), 1246-1267.
713 Miettinen, J., Shi, C., & Liew, S. C. (2016). Land cover distribution in the peatlands of
714 Peninsular Malaysia, Sumatra and Borneo in 2015 with changes since 1990. *Global*
715 *Ecology and Conservation*, 6, 67-78.

716 Milner, L. E. (2014). *Influence of fire on peat organic matter from Indonesian tropical*
717 *peatlands* (Doctoral dissertation, University of Leicester).
718 Moilanen, M., Hytönen, J., & Leppälä, M. (2012). Application of wood ash accelerates
719 soil respiration and tree growth on drained peatland. *European Journal of Soil*
720 *Science*, 63(4), 467-475.
721 Moore, S., Evans, C. D., Page, S. E., Garnett, M. H., Jones, T. G., Freeman, C., Hooijer,
722 A., Wiltshire, A. J., Limin, S. H., & Gauci, V. (2013) Deep instability of deforested
723 tropical peatlands revealed by fluvial organic carbon fluxes. *Nature*, 493, 660-664.
724 Murdiyarso, D., & Adiningsih, E. S. (2007). Climate anomalies, Indonesian vegetation
725 fires and terrestrial carbon emissions. *Mitigation and Adaptation Strategies for Global*
726 *Change*, 12(1), 101-112.
727 Neary, D. G., Klopatek, C. C., DeBano, L. F., & Ffolliott, P. F. (1999). Fire effects on
728 belowground sustainability: a review and synthesis. *Forest ecology and*
729 *management*, 122(1-2), 51-71.
730 Page, S. E., Siegert, F., Rieley, J. O., Boehm, H. D. V., Jaya, A., & Limin, S. (2002). The
731 amount of carbon released from peat and forest fires in Indonesia during
732 1997. *Nature*, *420*(6911), 61-65.
733 Page, S., Hosciło, A., Wösten, H., Jauhiainen, J., Silvius, M., Rieley, J., ... & Limin, S.
734 (2009). Restoration ecology of lowland tropical peatlands in Southeast Asia: current
735 knowledge and future research directions. *Ecosystems*, *12*(6), 888-905.
736 Page, S. E., Rieley, J. O., & Banks, C. J. (2011). Global and regional importance of the
737 tropical peatland carbon pool. *Global change biology*, *17*(2), 798-818.
738 Page, S. E., & Hooijer, A. (2016). In the line of fire: the peatlands of Southeast
739 Asia. *Philosophical Transactions of the Royal Society B: Biological*

740 *Sciences*, *371*(1696), 20150176.
741 Raj, R., Hamm, N. A. S., van der Tol, C., & Stein, A. (2016). Uncertainty analysis of gross
742 primary production partitioned from net ecosystem exchange
743 measurements. *Biogeosciences*, *13*(5).
744 Richardson, A. D., Hollinger, D. Y., Burba, G. G., Davis, K. J., Flanagan, L. B., Katul, G.
745 G., Munger, J. W., Ricciuto, D. M., Stoy, P. C., Suyker, A. E., Verma, S. B., & Wofsy,
746 S. C. (2006). A multi-site analysis of random error in tower-based measurement of
747 carbon and energy fluxes. *Agricultural and Forest Meteorology*, 136, 1-18.
748 Richardson, A. D., & Hollinger, D. Y. (2007). A method to estimate the additional
749 uncertainty in gap-filled NEE resulting from long gaps in the CO_2 flux record.
750 *Agricultural and Forest Meteorology*, 147, 199-208.
751 Smith, S. M., Newman, S., Garrett, P. B., & Leeds, J. A. (2001). Differential effects of
752 surface and peat fire on soil constituents in a degraded wetland of the northern Florida
753 Everglades. *Journal of Environmental Quality*, *30*(6), 1998-2005.
754 Stiegler, C., Meijide, A., Fan, Y., Ali, A. A., June, T. & Knohl, A. (2019). El Niño-
755 Southern Oscillation (ENSO) event reduces CO_2 uptake of an Indonesian oil palm
756 plantation. *Biogeosciences*, 16, 2873-2890.
757 Sundari, S., Hirano, T., Yamada, H., Kusin, K., & Limin, S. (2012). Effect of groundwater
758 level on soil respiration in tropical peat swamp forests. *Journal of Agricultural*
759 *Meteorology*, *68*(2), 121-134.
760 Taufik, M., Minasny, B., McBratney, A. B., Van Dam, J. C., Jones, P. D., & Van Lanen,
761 H. A. J. (2020). Human-induced changes in Indonesian peatlands increase drought
762 severity. *Environmental Research Letters*, *15*(8), 084013.
763 Thornley, J. H. M. (1976). Mathematical models in plant physiology: A quantitative

approach to problems in plant and crop physiology. London: Academic Press.

Toriyama, J., Takahashi, T., Nishimura, S., Sato, T., Monda, Y., Saito, H., Awaya, Y., Limin, S. H., Susanto, A. R., Darma, F, Krisyoyo, & Kiyono, Y. (2014). Estimation of fuel mass and its loss during a forest fire in peat swamp forests of Central Kalimantan, Indonesia. *Forest Ecology and Management*, 314, 1-8.

Ueyama, M., Hirata, R., Mano, M., Hamotani, K., Harazono, Y., Hirano, T., ... & Takahashi, Y. (2012). Influences of various calculation options on heat, water and carbon fluxes determined by open-and closed-path eddy covariance methods. *Tellus B: Chemical and Physical Meteorology*, *64*(1), 19048.

Ueyama, M., Iwata, H., Nagano, H., Tahara, N., Iwama, C., & Harazono, Y. (2019). Carbon dioxide balance in early-successional forests after forest fires in interior Alaska. *Agricultural and Forest Meteorology*, *275*, 196-207.

Vickers, D., & Mahrt, L. (1997). Quality control and flux sampling problems for tower and aircraft data. *Journal of atmospheric and oceanic technology*, *14*(3), 512-526.

Wakhid, N., Hirano, T., Okimoto, Y., Nurzakiah, S., & Nursyamsi, D. (2017). Soil carbon dioxide emissions from a rubber plantation on tropical peat. *Science of the total environment*, *581*, 857-865.

Ward, S. E., Ostle, N. J., Oakley, S., Quirk, H., Stott, A., Henrys, P. A., ... & Bardgett, R. D. (2012). Fire accelerates assimilation and transfer of photosynthetic carbon from plants to soil microbes in a northern peatland. *Ecosystems*, *15*(8), 1245-1257.

Webb, E. K., Pearman, G. I., & Leuning, R. (1980). Correction of flux measurements for density effects due to heat and water vapour transfer. *Quarterly Journal of the Royal Meteorological Society*, *106*(447), 85-100.

Wieder, R. K., Scott, K. D., Kamminga, K., Vile, M. A., Vitt, D. H., Bone, T., ... & Bhatti,

J. S. (2009). Postfire carbon balance in boreal bogs of Alberta, Canada. *Global Change Biology*, *15*(1), 63-81.

Figure legends

Fig. 1 Time-series photos of the study site: (a) November 2002, (b) April 2004, (c) June 2005, (d) September 2009 before fire, (e) October 2009 after fire, (f) December 2009, (g) December 2013 and (h) September 2014.

Fig. 2 Monthly variations in (a) precipitation, (b) GWL, (c) PPFD, (d) daytime (0900–1500) VPD and (e) CO_2 fluxes between 2000 and 2016, along with (f) EVI at 16-days intervals and (g) distance of hotspots from the flux tower within a circle of 5 km radius. EVI data were classified into two ranks according to reliability: useful or better (solid circles) and others (open circles). The red line denotes a moving average of seven consecutive solid circles. No data were available before March 2004 at the study site (grey area). As for precipitation and PPFD, data measured at a nearby forest site (DF) were shown for reference before April 2002. Dashed vertical lines denote the boundaries between three periods (refer to the text).

Fig. 3 Relationships of (a) measured RE (nighttime NEE) with GWL and (b) difference between RE and oxidative peat decomposition (PD) (measured nighttime RE – estimated PD from GWL) with GWL in Period I (April 2004 to September 2009), Period II (December 2009 to June 2014) and Period III (July 2014 to December 2016). Data in each period were binned equally into 15 classes according to GWL and averaged. Data except during fire in Period III are shown as grey circles. Error bars denote standard errors. Regression lines are drawn for original data if the regression is significant ($P < 0.05$).

Fig. 4 Interannual variation in measured RE (nighttime NEE) in high GWL conditions (≥ –0.2 m) between 2004 and 2016. Error bars denote standard errors.

Fig. 5 Interannual variation in GPP_{max} between 2004 and 2016. Error bars denote standard

errors.

Fig. 6 Relationships of light-saturated GPP at PPFD ≥ 1000 μmol m^{-2} s^{-1} (GPP_{1000}) with VPD in three GWL conditions in Period I (April 2004 to September 2009, a–c), Period II (December 2009 to June 2014, d–f) and Period III (July 2014 to December 2016, g–i). Data in each panel were binned equally into 15 classes according to VPD and averaged. Error bars denote standard errors.

Fig. 7 Cumulative CO_2 emissions including fire emissions from May 2004 to December 2016. Grey lines denote the events of fires and canal excavation.

824 Fig. 1

(a) November 2002

(b) April 2004

(c) June 2005

(d) September 2009

(e) October 2009

(f) December 2009

(g) December 2013

(h) September 2014

825

826 Fig. 2

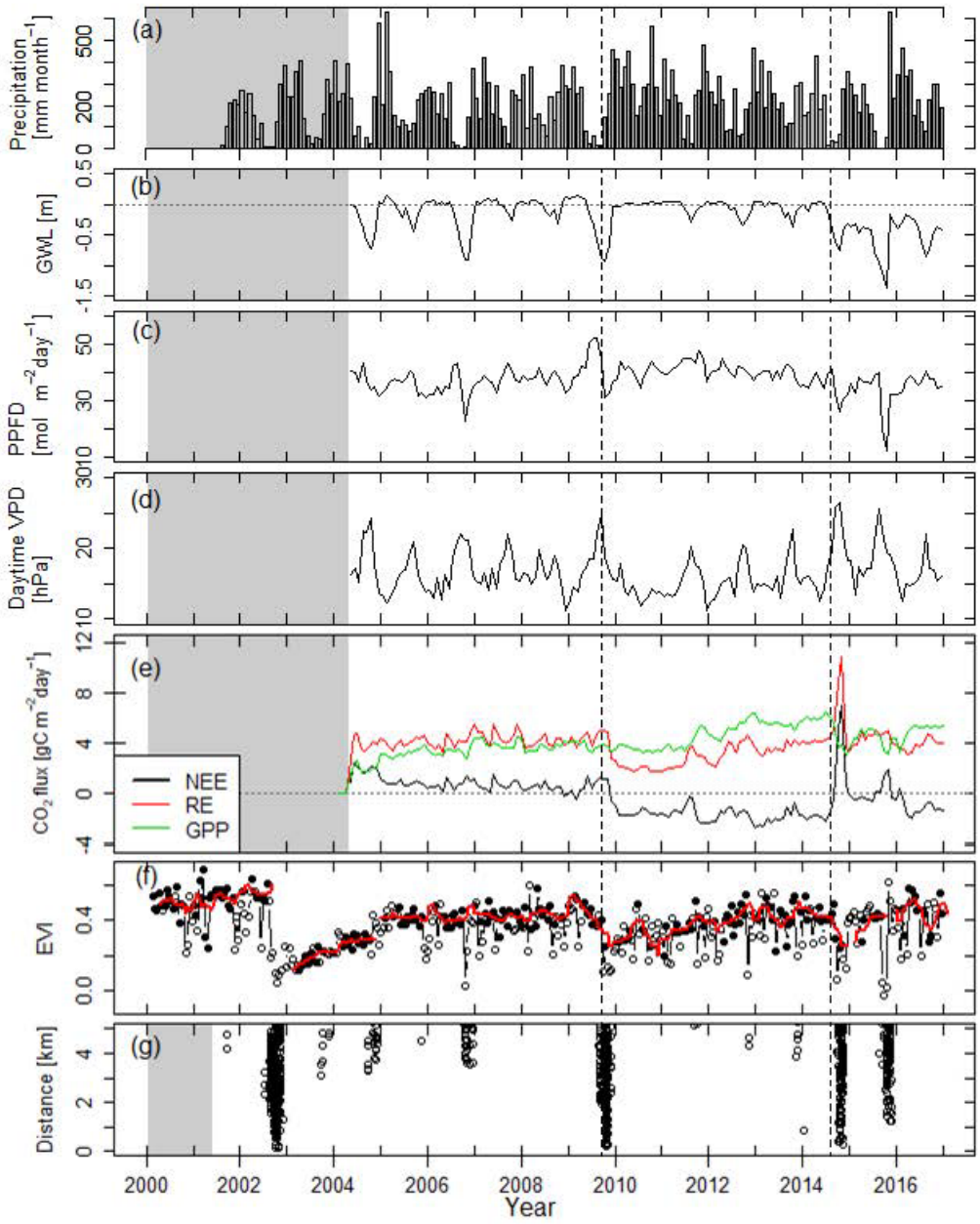

827

828

829 Fig. 3a

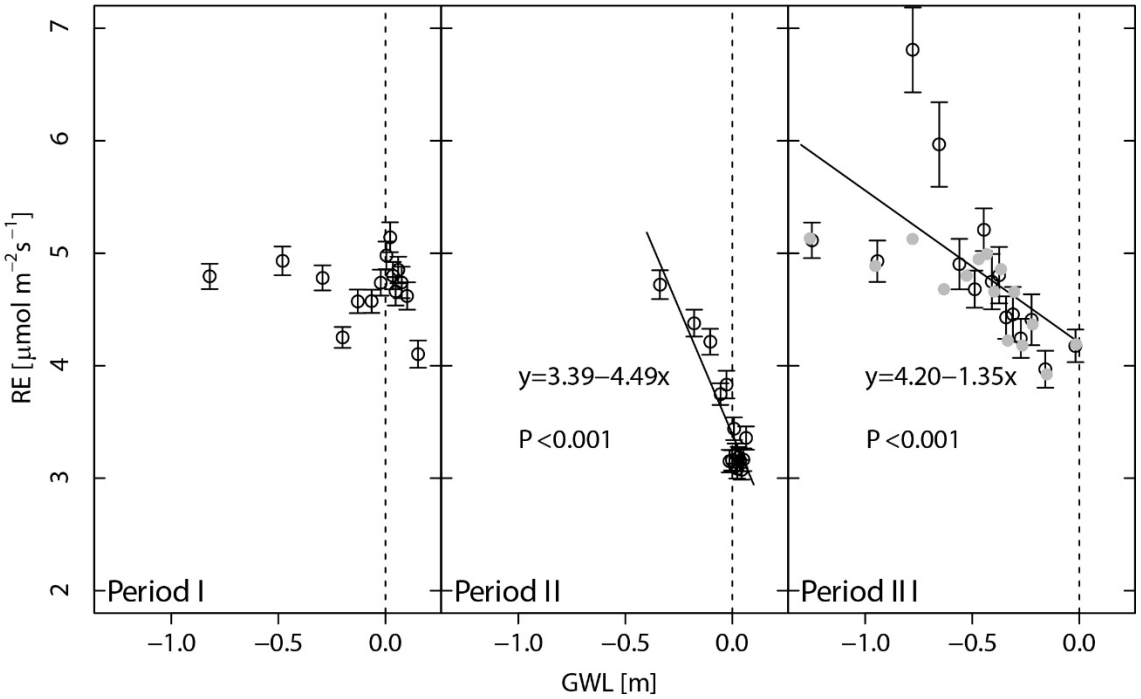

830

831 Fig. 3b

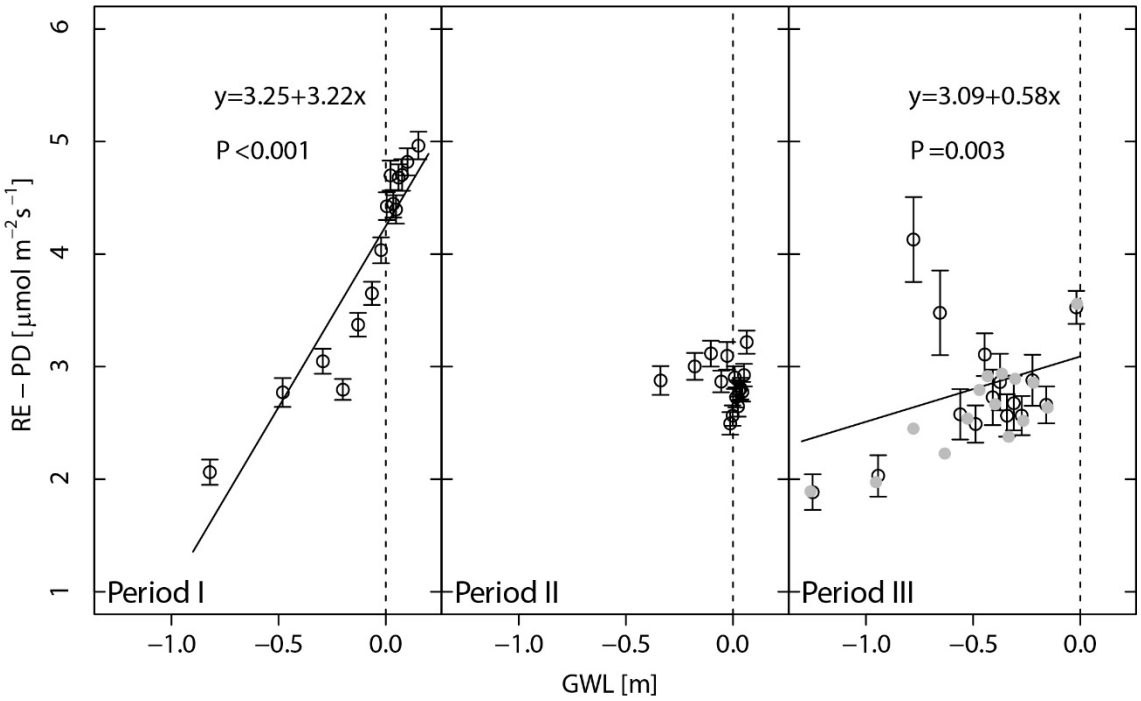

832

833

834 Fig. 4

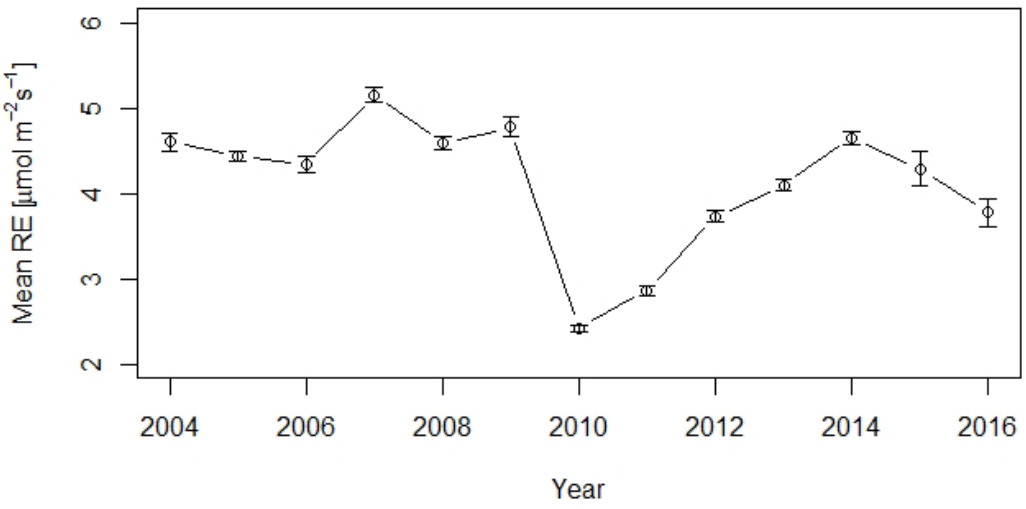

835

836

837 Fig. 5

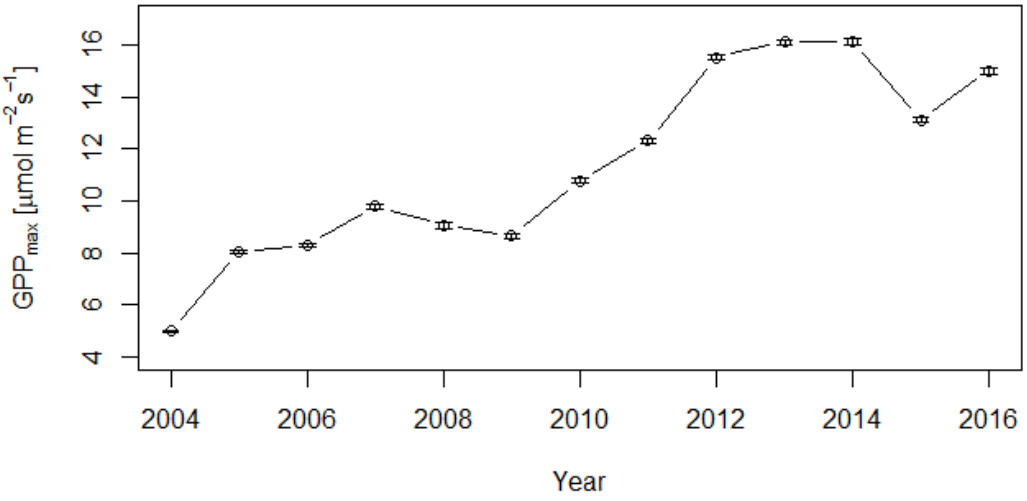

838

839

840 Fig. 6

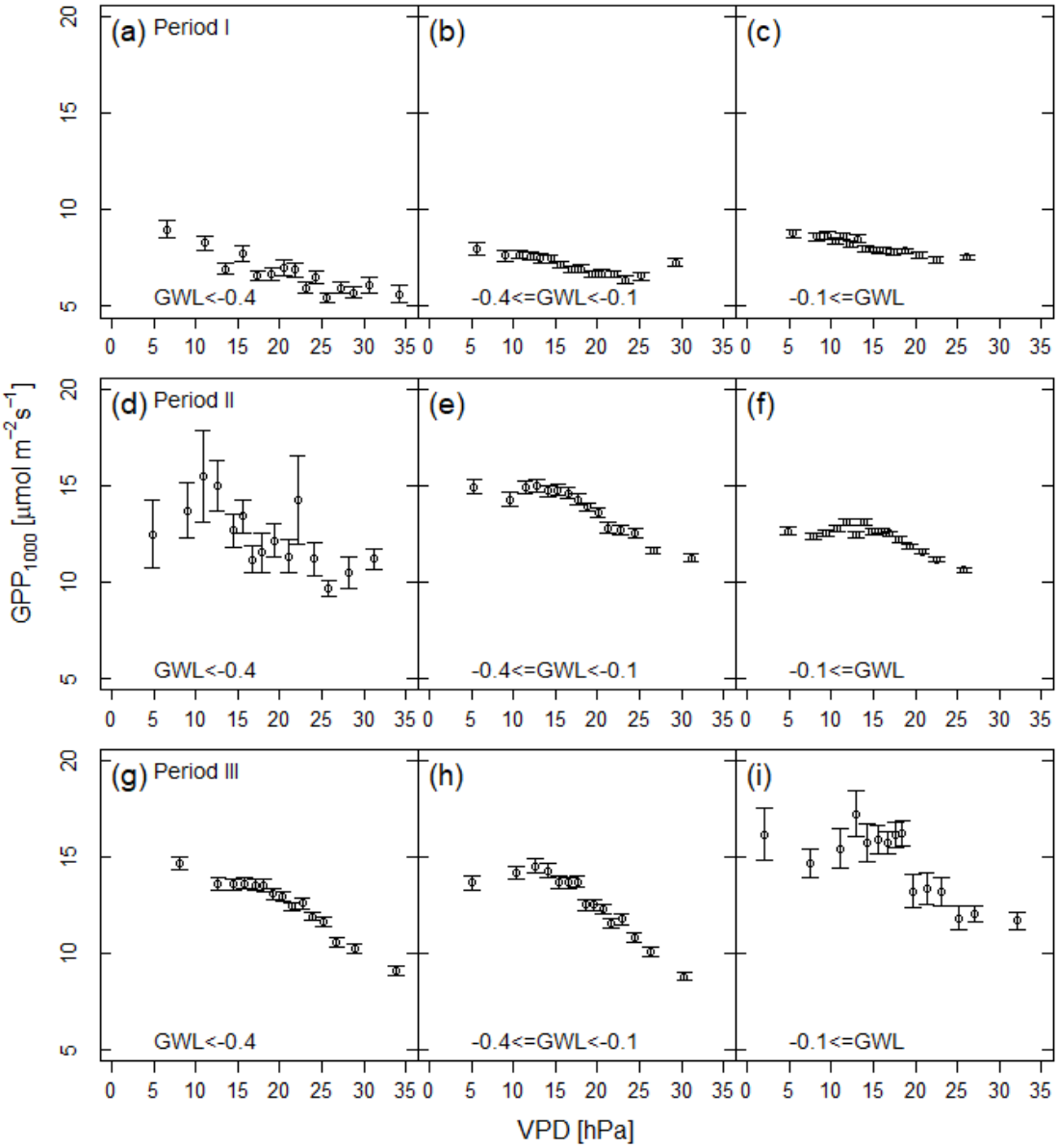

841

842

843 Fig. 7

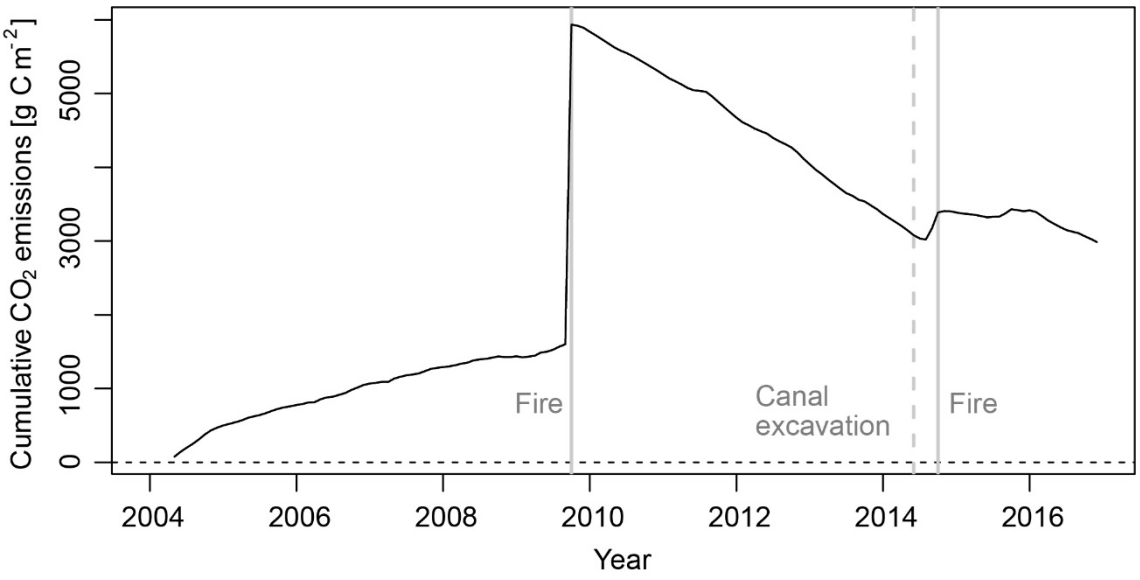
Cumulative CO_2 emissions [g C m^{-2}]
0
1000
3000
5000
2004
2006
2008
2010
2012
2014
2016
Year
Fire
Canal excavation
Fire

844

Tables

Table 1. Annual values of CO_2 fluxes and environmental factors.

Year	2005	2006	2007	2008	2009	2010	2011	2012	2013	2014	2015	2016
NEE (g C m^{-2} yr^{-1})[a]	290 (17)	290 (32)	231 (27)	147 (31)	163 (42)	−577 (9)	−570 (16)	−629 (14)	−684 (14)	−28 (34)	1 (18)	−381 (21)
RE (g C m^{-2} yr^{-1})[a]	1487 (20)	1528 (39)	1692 (24)	1488 (25)	1544 (42)	715 (13)	957 (23)	1308 (23)	1343 (22)	1870 (50)	1634 (31)	1428 (32)
PD (g C m^{-2} yr^{-1})	333	466	192	256	464	201	259	333	301	483	844	749
RE−PD (g C m^{-2} yr^{-1})	1155	1062	1500	1232	1080	514	698	975	1042	1386	790	679
GPP (g C m^{-2} yr^{-1})[a]	1197 (13)	1238 (23)	1461 (26)	1341 (35)	1380 (35)	1292 (10)	1527 (18)	1937 (19)	2027 (16)	1898 (25)	1633 (19)	1809 (22)
GWL (m)	−0.08	−0.25	0.00	−0.03	−0.25	0.01	−0.04	−0.08	−0.06	−0.22	−0.59	−0.43
Minimum monthly GWL (m)	−0.44	−0.92	−0.28	−0.32	−0.93	−0.03	−0.30	−0.33	−0.36	−0.74	−1.38	−0.85
Precipitation (mm yr^{-1})	2620	1977	2555	2603	2239	3750	3021	2460	2776	2220	2388	3077
PPFD (kmol m^{-2} yr^{-1})	13.0	12.5	13.8	13.9	15.1	14.7	15.6	14.9	14.4	12.8	11.9	13.4
Daytime VPD (hPa)[b]	15.6	17.2	16.8	16.2	17.5	13.9	15.3	15.5	16.0	18.1	18.8	16.0
Ratio of daytime VPD > 15 hPa[b]	0.56	0.61	0.64	0.59	0.65	0.43	0.53	0.55	0.57	0.66	0.72	0.59
EVI	0.414	0.427	0.422	0.429	0.411	0.310	0.361	0.412	0.431	0.386	0.385	0.444

[a] Uncertainty due to random errors is shown in parentheses.

[b] Data in the daytime (0900–1500).

Table 2.

Mean values (± 1 standard deviation) of CO_2 fluxes and environmental factors in the three periods of 2005–2008, 2010–2013 and 2015–2016. The *P* values of one-way ANOVA were also shown. Different letters in the same row denote significant difference among periods ($P < 0.05$) according to Tukey's HSD.

Year	2005–2008	2010–2013	2015–2016	ANOVA (*P*)
NEE (g C m^{-2} yr^{-1})	240±68a	−615±53c	−190±270b	<0.001
RE (g C m^{-2} yr^{-1})	1549±97a	1081±300b	1531±146ab	0.035
PD (g C m^{-2} yr^{-1})	312±118a	274±57a	794±67b	<0.001
RE−PD (g C m^{-2} yr^{-1})	1237±188a	807±246b	735±78ab	0.031
GPP (g C m^{-2} yr^{-1})	1309±118a	1696±346a	1721±124a	0.106
GWL (m)	−0.09±0.11a	−0.04±0.04a	−0.51±0.11b	0.001
Minimum monthly GWL (m)	−0.49±0.29ab	−0.26±0.15b	−1.12±0.37a	0.019
Precipitation (mm yr^{-1})	2339±309a	3002±549a	2733±487a	0.276
PPFD (kmol m^{-2} yr^{-1})	13.3±0.67ab	14.9±0.51b	12.7±01.06a	0.011
Daytime VPD (hPa)[a]	16.5±0.70a	15.2±0.90a	17.4±1.98a	0.100
Daytime ratio of VPD>15 hPa[a]	0.60±0.03a	0.52±0.06a	0.66±0.09a	0.067

853 [a] Data in the daytime (0900–1500).